Injection of electron beam into a toroidal trap using chaotic orbits near magnetic null

C. Nakashima,[1,*] Z. Yoshida,[2] H. Himura,[2] M. Fukao,[3] J. Morikawa,[3] and H. Saitoh[2]
[1]*Graduate School of Engineering, The University of Tokyo, 7-3-1 Hongo, Bunkyo-ku, Tokyo 113-0033, Japan*
[2]*Graduate School of Frontier Sciences, The University of Tokyo, 7-3-1 Hongo, Bunkyo-ku, Tokyo 113-0033, Japan*
[3]*High Temperature Plasma Center, The University of Tokyo, 7-3-1 Hongo, Bunkyo-ku, Tokyo 113-0033, Japan*
(Received 23 August 2001; published 21 February 2002)

Injection of charged particle beam into a toroidal magnetic trap enables a variety of interesting experiments on non-neutral plasmas. Stationary radial electric field has been produced in a toroidal geometry by injecting electrons continuously. When an electron gun is placed near an *X* point of magnetic separatrix, the electron beam spreads efficiently through chaotic orbits, and electrons distribute densely in the torus. The current returning back to the gun can be minimized less than 1% of the total emission.

DOI: 10.1103/PhysRevE.65.036409 PACS number(s): 52.27.Jt, 52.20.Dq, 52.65.Cc

I. INTRODUCTION

A variety of applications of non-neutral plasmas are attracting much interest. Conventional methods of trapping charged particles use both magnetic and electric fields to confine particles in a linear geometry [1]. Other possibilities are the use of toroidal geometry where endless magnetic-field lines in the confinement region can achieve pure magnetic confinement. Some different toroidal systems have been developed for heavy-ion accelerators [2,3], electrostatic thermonuclear fusion reactors [4,5], non-neutral beam equilibria [6], and production and confinement of toroidal electron plasmas [2,7–10]. Recently, a type of toroidal magnetic trap has been developed aiming at production of antimatter plasmas [11] and high-β fusion plasmas [12–14].

One of the key issues in developing a particle trap is how we can inject particles into the confinement region. Unlike gas-discharge production of neutral plasmas, particles are generated outside the trap in order to avoid particle loss due to the interaction of particles (such as antimatter particles) with their source. In a linear system, particles are injected by opening the plugging electric potential. This method cannot be used in a toroidal system that does not have open ends of field lines. In earlier experiments, some different methods of injection were invented. The inductive charging method [2] injects electron-loaded magnetic flux tubes with rising the toroidal magnetic field. In a stationary magnetic field, one can use the drift motion of particles with the help of a spatial nonuniform toroidal magnetic field combined with external and self-generated electric fields [9].

This paper describes a simple injection scheme that can produce a sufficiently large floating potential. A merit of toroidal geometry in this scheme is that the connection lengths (the lengths between the source and sinks of the particles) can be made much longer than the size of the device if particles describe chaotic orbits near a separatrix (a magnetic surface with null points) [11]. Continuous injection of particles through the long orbits enables steady-state operation of the trap. The separatrix separates the trapping region and the particle source. In Sec. II, we describe the system of the toroidal trap with an internal ring conductor. In order to find optimum parameters for injection, we calculated orbits of electrons (Sec. III). Experimental results are given in Sec. IV and compared with the numerical calculation results in Sec. V.

II. TOROIDAL TRAP WITH MAGNETIC SHEAR CONFIGURATION

Demonstration of electron-beam injection into a toroidal system was done on the Prototype Ring Trap (Proto-RT) device (Fig. 1). The details of the Proto-RT can be found in Ref. [15]. Typical parameters of the experiment are listed in Table I. An internal ring conductor (30 cm major radius and 4.3 cm minor radius) is installed in a vacuum vessel (59 cm inner radius and 90 cm height). The ring conductor is supported by eight rods (3 mm diameter) and magnetized by feeding current through two tubes (~ 3 cm diameter). A ceramic tube covers each structure. The vacuum chamber is evacuated to $\sim 3\times 10^{-7}$ Torr. The casing of the internal ring conductor and the vacuum chamber are grounded electrically through low impedance registers (100Ω). Particles are trapped primarily by a stationary poloidal magnetic field (B_p) with a separatrix (shown in Fig. 1), that is produced by combination of a dipole field generated by the ring conductor and a vertical field. We can add a stationary toroidal magnetic field (B_t) to produce magnetic shear that effectively stabilizes electrostatic instabilities [16]. The combination of B_p and B_t can also adjust the orbits of injected electrons to increase the connection lengths [17]. Electrons are injected continuously ($\sim 10^2$ sec) from an electron gun that uses a heated 2%-thoriated tungsten wire ($\phi \sim 0.3$ mm) and can accelerate electrons up to 2 keV. The diameter of the anode aperture is 4 mm. The direction of the injection is 0° with respect to the horizontal plane ($Z=0$) and 11° inward with respect to the toroidal tangent as shown in Fig. 1. The electron-beam current is about 10 mA. The casing of the electron gun is floated electrically in normal operation. To measure a potential, electrostatic probes (#1-#3; shown in Fig. 1) are inserted into the plasma at three different toroidal positions (60°, 180°, and 300° from the electron gun) on the

*Electronic address: nakasima@plasma.q.t.u-tokyo.ac.jp

 ©2002 The American Physical Society

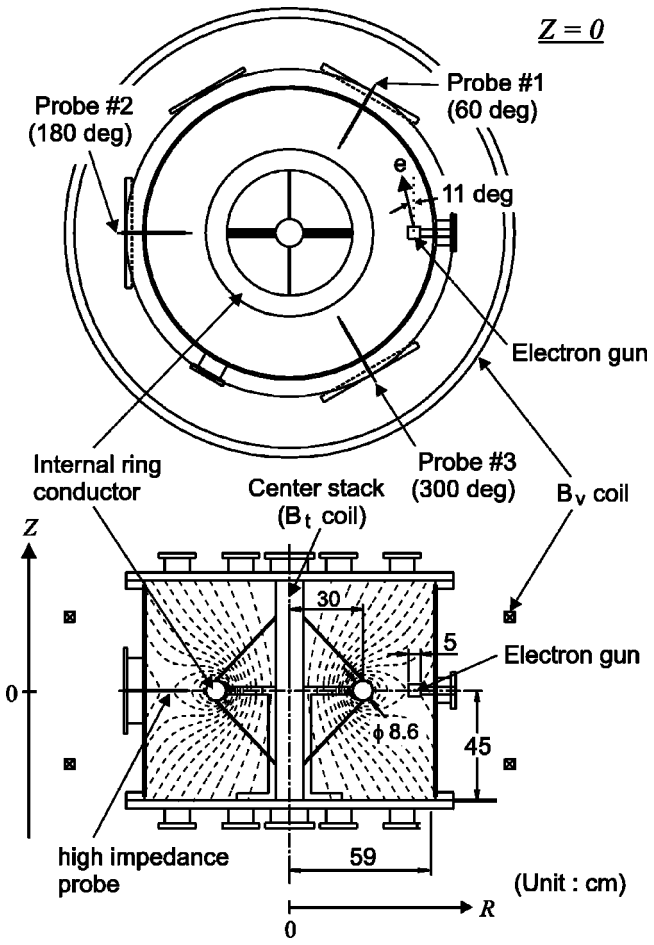

FIG. 1. Schematic view of the Proto-RT device.

horizontal plane ($Z=0$). Each cylindrical probe has 1.0 mm diameter and 1.5 mm length. The floating potential (Φ) is estimated at high impedance of order $10^9\Omega$.

III. ORBIT OPTIMIZATION FOR INJECTION

For the optimization of orbits to inject electrons, we analyzed the particle motion numerically. In Fig. 2(a) we show

TABLE I. Typical parameters of electron injection experiments.

Vacuum vessel	inner radius	59 cm
	height	90 cm
	vacuum	$\sim 3\times 10^{-7}$ Torr.
Internal ring	major radius	30 cm
	minor radius	4.3 cm
	coil current	7.875 kAT
Vertical field coil	radius	90 cm
	coil current	2.1 kAT
Toroidal field coils	coil current	0.78 kAT
Magnetic field	poloidal	~ 40 G
(at $R=42$ cm)	toroidal	~ 3 G
Electron gun	acceleration voltage	2 kV
	beam current	~ 10 mA
	diameter of aperture	4 mm
	(injection) pitch angle	$\sim 11°$

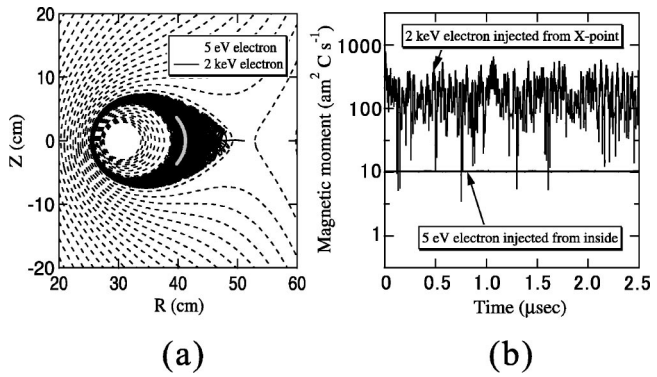

FIG. 2. (a) Calculated typical orbits of 2 keV (black-solid curve) and 5 eV (gray-solid curve) electrons (projections on a poloidal cross section) and typical magnetic surfaces (dashed curves). (b) Calculated time evolution of the magnetic moment (μ) of the electrons [2 keV and 5 eV electrons shown in (a)]. The vertical axis has a logarithmic scale with the base of 10. Nonconservation of μ is essential to obtaining chaotic orbits.

the projections, onto a poloidal cross section, of typical orbits of 2 keV (black-solid curve) and 5 eV (gray-solid curve) electrons in comparison with magnetic surfaces (dashed curves). When electrons come back to the source (with the size $\sim 5\times 5\times 5$ cm) or hit the boundary of the chamber, the orbit calculation is terminated.

High-energy (2 keV) electrons injected through the separatrix have long orbits covering almost densely the trapping region. The pitch angle between the injection direction and the magnetic field line is about 11° near the X point where $B_p \approx 0$. The electron is emitted from $R=51.25$ cm (0.25 cm outside the X point). The gyroradius is of order 10 cm. The staying time of the beam electron (2 keV) in the trapping region is about 3 μsec and the corresponding connection length is about 70 m. This orbit is compared with that of a 5 eV electron injected from 10 cm inside the separatrix. A low-energy electron is magnetized in the trapping region and moves on a magnetic surface. In Fig. 2(b), we plot the time evolution of the magnetic moment (μ) of both 2 keV and 5 eV electrons. For a magnetized low-energy electron, μ is conserved. For a high-energy electron, μ changes almost randomly. Nonconservation of μ is essential to obtain chaotic orbits. In the present calculations, we neglect the effect of the self-electric field generated by trapped electrons. For low-energy magnetized particles, the self-electric field helps to confine them; the $\boldsymbol{E}\times\boldsymbol{B}$ drift overcomes the curvature and gradient $\boldsymbol{B}$ drifts [2,7–9].

In Fig. 3, we compare orbits (toroidal projections) starting from different positions; (a) $R_{gun}=49.0$ cm, (b) $R_{gun}=51.3$ cm, and (c) $R_{gun}=51.2$ cm. When the electron source is placed inside the separatrix [Fig. 3(a)], the electron moves in the toroidal direction and comes back to the electron source. When the source is placed outside the X point [Fig. 3(b)], the electron is not injected into the trapping region and lost immediately. If the source is placed near the X point [Fig. 3(c)], the electron describes a chaotic and long orbit before it comes back to the source. Near the X point, the orbit of the electron has a very strong and almost random

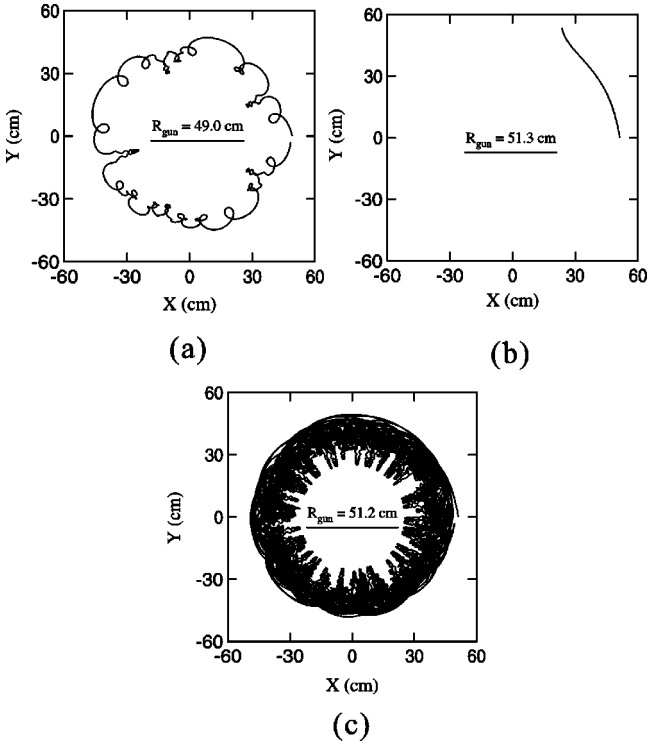

FIG. 3. Calculated orbits starting from different positions; (a) $R_{gun}=49.0$ cm, (b) $R_{gun}=51.3$ cm, and (c) $R_{gun}=51.2$ cm. The electron emitted near the X point describe a chaotic and long orbit before it comes back to the source.

dependence on the initial position because of the chaos of the electron motion.

IV. ELECTRON INJECTION EXPERIMENT

Using the parameters determined by the numerical orbit analysis (Sec. III), we injected electrons with energy of 2 keV. Figure 4 shows the floating potential (Φ) measured at $R=42.0$ cm by the probe #2 (toroidal angle 180° from the electron gun) as a function of the radial position of the electron gun. Two cases of magnetic-field configurations are compared. The black points show the potential Φ in an optimized magnetic field ($B_p>0$) based on the orbit calculations in the previous section. The maximum value of the Φ is about -65 V at $R=42.0$ cm, when the gun is deeply inserted into the trapping region ($R_{gun}=42.0$ cm) and the beam current is about 10 mA. When the electron gun is placed at $R=51.0$ cm (near the X point) the value of the Φ (at $R=42.0$ cm) is about -35 V (about 50% of the maximum value). If we flip the sign of the poloidal magnetic field ($B_p<0$), the Φ decreases (white square markers). In this case, the value of the Φ (at $R=42.0$ cm) is about -10 V when the electron gun is placed inside the separatrix ($R_{gun}=36.0$–47.0 cm). Thus, we could inject electrons efficiently from the neighborhood of the X point (the edge of the trapping region) into the trapping region (inside the separatrix).

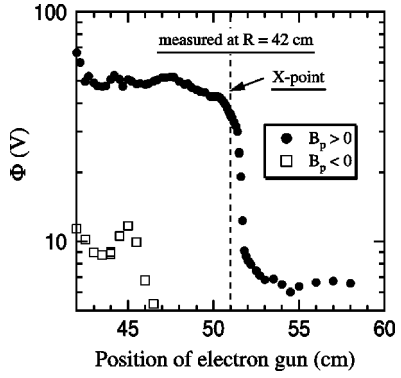

FIG. 4. Measured floating potential at $(R,Z)=(42$ cm,0) (inside the trapping region) as a function of the position of the electron gun The vertical axis has a logarithmic scale with the base of 10. Electrons can be injected effectively in the optimized magnetic configuration (black points). If the sign of the B_p is flipped (white-square markers), the potential decreases.

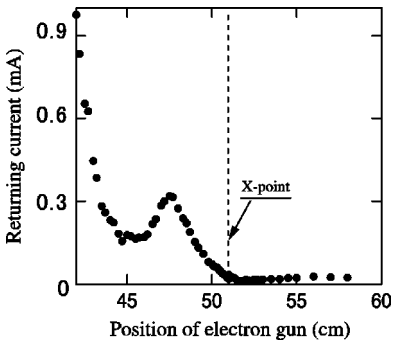

FIG. 5. Measured loss current collected by the casing of the electron gun; we can reduce the particle (flux) loss to the electron gun (less than 1% of the total emission) by locating the gun near the X point.

Figure 5 shows the loss current collected by the grounded casing of the electron gun as a function of the radial position of the gun. The maximum value of the loss current is ~ 1 mA (about 10% of the total emission), when the gun is deeply inserted inside the separatrix. When the electron gun is located near the X point, the loss current decreases, probably due to the effect of the chaotic orbits. In this case, the value of the loss current is ~ 0.02 mA (less than 1% of the total emission and about 2% of the maximum value, which is compared with the decrease in Φ in Fig. 4).

Radial floating potential profiles are measured by high-impedance probes. In Fig. 6, we show the potential profiles at three different toroidal positions (60°, 180°, and 300° from the electron gun) on the horizontal plane ($Z=0$). Here, the electron gun is placed near the X point ($R=51.2$ cm) with the optimized injection angle. The potential profiles have approximately broad parts inside the trapping region (36 cm$\lesssim R\lesssim$51 cm). Toroidally asymmetric peaks are considered to be corresponding to the beam (the measured potential includes the kinetic-energy part of the Hamiltonian). From the data obtained at 60° (by the probe #1) a peak appears around $R=50.5$ cm, and at 180° (by the probe #2) two large peaks appear inside the separatrix (at $R=39.5$ and 46.5 cm). At 300° (by the probe #3), far from the electron gun, we do not observe large peaks, which implies that the mixing effect of chaos has randomized the beam orbits.

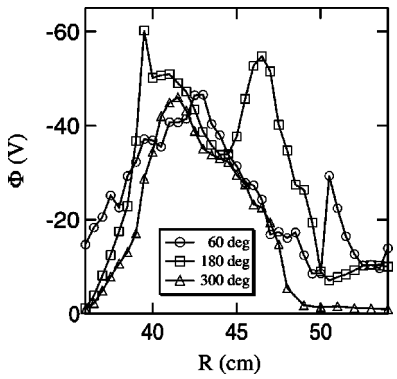

FIG. 6. Measured radial floating potential profiles at three different toroidal positions (60°, 180°, and 300° from the electron gun) on the horizontal plane ($Z=0$). Toroidally asymmetric peaks are considered to be corresponding to the beam.

In Fig. 7, we show the potential profiles for different B_t. If the toroidal magnetic field is weak ($\lesssim 20$ G), the potential buildup inside the trapping region with broad radial profiles. The maximum value of the potential is about -40 V (at $R \sim 41$ cm), when $B_t \sim 3.4$ G. For larger $B_t (\gtrsim 50$ G) we observe only beams near the X point ($R=51$ cm), which implies that electrons are magnetized by the strong B_t and they cannot be injected into the trapping region.

V. DISCUSSION

We discuss the experimental results comparing with the numerical orbit analyses. Figure 8 shows the calculated staying time of beam electrons as a function of the initial position of injection. The calculation is terminated when the electron hits the source (electron gun) or the boundary. In the experiment, the divergence angle of the electron beam is about 20°. To estimate average orbit lengths, we compare different injection angles; (a) 0°, ±5.7°, and ±11.3° with respect to the horizontal plane, (b) 0°, −5.7°, −11.3°, −16.7°, and −21.8° with respect to the toroidal direction. Electrons have three types of orbits with respect to the initial position of injection; (A) magnetized orbits inside the separatrix, (B) chaotic orbits near the X point, (C) escaping orbits outside the separatrix. In the case of (A), electrons emitted from the source (placed in the strong-field region) return to their source after a few gyrations. Very short staying time ($\lesssim 10^{-8}$ sec) occurs for such orbits when the source is placed deeply inside the separatrix ($R_{gun} \lesssim 46$ cm). In the case o f (B), electrons emitted from the source (placed in the weak-field region; 48 cm$\lesssim R_{gun} \lesssim$51 cm) come back to their source or escape from the trapping region near the X point. The staying time of electrons has a very strong and almost random dependence on the initial condition of the orbit because of the chaos of the electron motion. In the case of (C), electrons are not trapped and lost directly at the wall. In Fig. 9, we summarize the results of calculations with diverse injection conditions [with regard to the horizontal angle (white circle markers) and the radial angle (white diamond markers)], which is compared with the experimental result (Fig. 4).

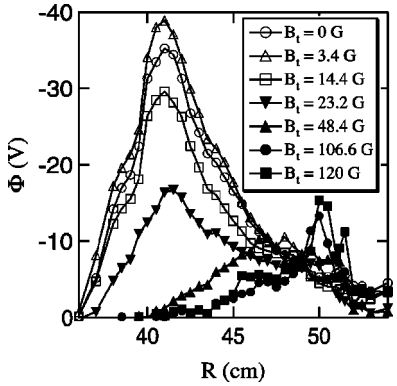

FIG. 7. Measured radial floating potential profiles for the different B_t; if the toroidal magnetic field is weak ($\lesssim 20$ G), the potential builds up inside the trapping region. For larger $B_t (\gtrsim 50$ G), we observe only beams near the X point (at $R=51$ cm).

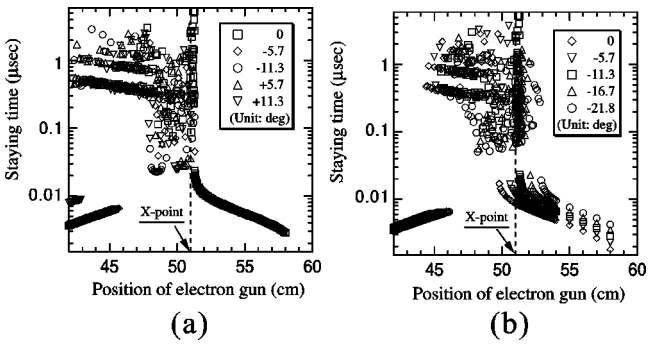

FIG. 8. Calculated staying time of beam electrons as a function of the initial position with the injection angle (a) 0°, ±5.7°, and ±11.3° with respect to the horizontal plane, (b) 0°, −5.7°, and −11.3°, −16.7°, and −21.8° with respect to the toroidal direction. The vertical axes of both figures (a) and (b) have logarithmic scales with the base of 10.

We made further detailed studies on the injection conditions. In Fig. 10, we compare different injection angles of the electron gun with respect to the horizontal directions. Figure 10(a) is the plot of calculated staying time of beam electrons

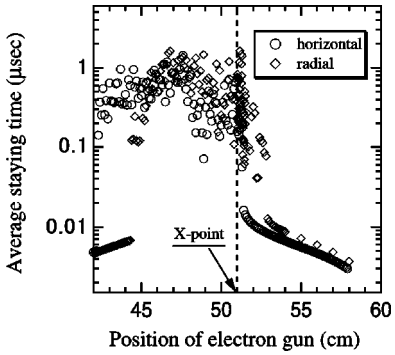

FIG. 9. Calculated average staying time of beam electrons (from the results in Fig. 8) vs the initial position of injection, which is compared with the experimental result (Fig. 4). The vertical axis has a logarithmic scale with the base of 10.

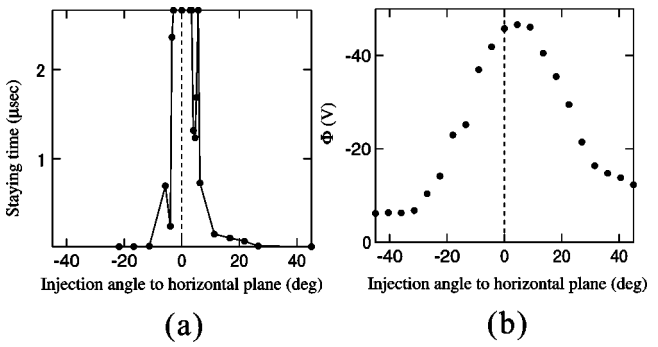

FIG. 10. (a) Calculated staying time of beam electrons vs injection angle with respect to the horizontal plane ($Z=0$). (b) Measured floating potential (at $R=41$ cm) vs injection angle with respect to the horizontal plane.

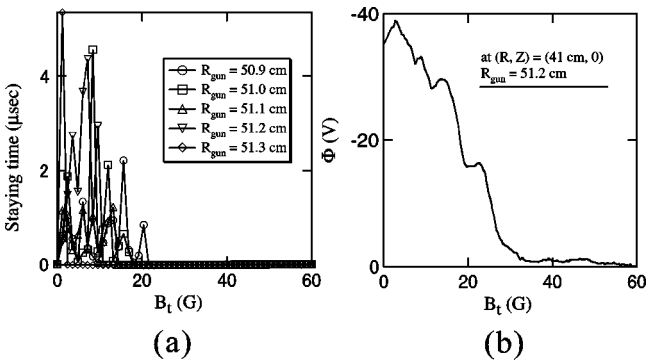

FIG. 11. (a) Calculated staying time of beam electrons (starting from different positions; $R=50.9,51.0,51.1,51.2$, and 51.3 cm) vs toroidal magnetic-field strength. (b) Measured floating potential (at $R=41$ cm) vs toroidal magnetic-field strength.

and Fig. 10(b) is the measured floating potential (at $R=41$ cm). The electron gun is placed at $R=51$ cm (near the X point). We found numerically and experimentally that the injection is optimized when the injection angle is $\sim 5°$ with respect to the horizontal plane. Figures 11(a) and 11(b) are the calculated staying time of beam electrons (starting from different positions; $R=50.9,51.0,51.1,51.2$, and 51.3 cm and the measured floating potential (at $R=41$ cm) as a function of the toroidal magnetic field, respectively. With keeping the poloidal magnetic field constant, we changed the toroidal magnetic field (B_t). For $B_t \gtrsim 20$ G, electrons come back to their source soon with short staying time [Fig. 11(a)]. Also, in the experiment [Fig. 11(b)], the potential decreases for $B_t \gtrsim 20$ G.

Finally, we can estimate the total charge Q_{cal} of trapped electrons by the relation $Q_{cal}=I_{inj}\times\tau_{trap}$ (I_{inj} is the injected beam current, τ_{trap} is the average staying time of beam electrons). When the source is placed inside the separatrix (46 cm$\lesssim R_{gun} \lesssim$48 cm) we estimate, by orbit analysis, the average staying time to be of order 10^{-6} sec. For $I_{inj}\simeq 8$ mA (experimental condition), the total charge is estimated to be about 8 nC. On the other hand, the experimentally stored charge can be related with the potential by the Poisson equation that is approximated by $Q_{est}\approx 8\pi^2 R\epsilon_0\Phi$ (R is the major radius). Using experimental values $R=0.42$ m and $\Phi\sim -50$ V, we obtain $Q_{est}\sim 15$ nC. The trapped charge Q_{est} is larger than Q_{cal} by factor 2, which may imply the existence of thermalized electrons. The electron temperature of the bulk component has been measured by Langmuir probes. The typical temperature of the electron plasma has estimated to be about 60 eV [17].

VI. SUMMARY

We have studied the injection conditions of electrons into a toroidal magnetic trap system. Development of a particle injection scheme is an essential issue in the study of toroidal (closed magnetic surfaces) non-neutral plasmas. Particles need long orbit lengths to break the conservation of the angular momentum and cross magnetic surfaces toward the confinement region. Chaotic (nonintegrable) orbits can have long orbit lengths (connection length). We found appropriate conditions to inject nonmagnetized electrons near the edge of the trapping region. Experimental tests have shown good agreements with the numerical optimization of the position, the angle of injection, and magnetic-field configuration. The current coming back to the gun can be minimized below 1% of the emitted current. By measuring the radial profile of the floating potential, we found two components; one is a broad symmetric part of distribution and the other is a narrow nonsymmetric peak corresponding to the beam. In the present experiment, the plasma is dominated by beam components (the potential is consistent to the average staying time of the beam electrons). To thermalize and confine particles more efficiently, we can apply radio frequency electric field to break the conservation of the canonical angular momentum [18]. This will be reported elsewhere.

ACKNOWLEDGMENTS

The authors are grateful to Professor T. M. O'Neil, UCSD non-neutral plasma group, Professor Yuichi Ogawa, and Dr. Shigeo Kondoh for their suggestions and discussions. This work was supported by Grant-in-Aid for Scientific Research from the Japanese Ministry of Education, Science and Culture No. 09308011.

[1] D.H. Dubin and T.M. O'Neil, Rev. Mod. Phys. **71**, 87 (1999).
[2] J.D. Daugherty, J.E. Eninger, and G.S. Janes, Phys. Fluids **12**, 2677 (1969).
[3] N. Rostoker, Part. Accel. **5**, 93 (1973).
[4] T.H. Stix, Phys. Rev. Lett. **24**, 135 (1970).
[5] N.G. Popkov, Sov. J. Plasma Phys. **5(4)**, 482 (1979).
[6] A. Mohri, M. Masuzaki, T. Tsuzuki, and K. Ikuta, Phys. Rev. Lett. **34**, 574 (1975).
[7] W. Clark, P. Korn, A. Mondelli, and N. Rostoker, Phys. Rev. Lett. **37**, 592 (1976).
[8] P. Zaveri, P.I. John, K. Avinash, and P.K. Kaw, Phys. Rev. Lett. **68**, 3295 (1992).

[9] S.S. Khirwadkar, P.I. John, K. Avinash, A.K. Agarwal, and P.K. Kaw, Phys. Rev. Lett. **71**, 4334 (1993).
[10] C. Nakashima *et al.*, in Proceedings of the International Congress on Plasma Physics, Quebec City, 2000, Vol. 1, p. 112.
[11] S. Kondoh and Z. Yoshida, Nucl. Instrum. Methods Phys. Res. A **382**, 561 (1996).
[12] S.M. Mahajan and Z. Yoshida, Phys. Rev. Lett. **81**, 4863 (1998).
[13] Z. Yoshida *et al.*, in *Proceedings of Non-neutral Plasma Physics III*, edited by J. Bollinger, R. Spencer, and R. Davidson, AIP Conf. Proc. No. 498 (AIP, New York, 1999), p. 398.
[14] H. Himura, *et al.*, in Fusion Energy 2001, 18th IAEA Fusion Energy Conference, Sorrento, Italy (International Atomic Energy Agency, Vienna, in press), paper no. IAEA-CN-77-ICP/14.
[15] H. Himura *et al.*, in *Proceedings of Non-neutral Plasma Physics III*, edited by J. Bollinger, R. Spencer, and R. Davidson, AIP Conf. Proc. No. 498 (AIP, New York, 1999), p. 405.
[16] S. Kondoh, T. Tatsuno, and Z. Yoshida, Phys. Plasmas **8**, 2635 (2001).
[17] C. Nakashima *et al.*, in *Proceedings of Non-neutral Plasma Physics III*, edited by J. Bollinger, R. Spencer, and R. Davidson, AIP Conf. Proc. No. 498 (AIP, New York, 1999), p. 411.
[18] C. Nakashima and Z. Yoshida, Nucl. Instrum. Methods Phys. Res. A **428**, 284 (1999).